Measurement of the refractive index of electrically poled soda-lime glass layers using leaky modes

ROBERT OVEN*

School of Engineering and Digital Arts, The University of Kent, Canterbury, Kent, UK, CT2 7NT

**Corresponding author: R.Oven@kent.ac.uk*

Received XX Month XXXX; revised XX Month, XXXX; accepted XX Month XXXX; posted XX Month XXXX (Doc. ID XXXXX); published XX Month XXXX

Electrically poled layers have been formed in soda-lime glass using graphite electrodes in air. The refractive index and thickness of the poled glass layers have been measured by the analysis of leaky optical modes. These modes are supported by the poled layer and can be determined by analysis of the optical reflectivity measured with a prism coupler arrangement. A relatively constant refractive index ~ 1.486 in the poled glass region is measured, which is ~0.03 below the substrate index. The reflectivity data shows that the transition between poled and un-poled glass is very sharp and is consistent with ion transport models. The thickness of the poled glass region is consistent with the removal of Na^+ and K^+ ions from the poled region. The index and depth data is confirmed by interferometric measurements. The tensile stress in the poled glass layer is also estimated from optical birefringence measurements and is estimated to be ~0.3 GN/m^2. © 2016 Optical Society of America

OCIS codes: *(160.2900) Glass and other amorphous materials; (160.3130) Integrated optics materials; (130.2755) Glass waveguides.*

http://dx.doi.org/10.1364/AO.99.099999

1. INTRODUCTION

Electrically poled glass has received considerable interest in the literature in recent years, not least due to the observation of a second order non-linearity in its refractive index [1-5]. These effects have been observed in many glasses including silica glass and soft soda-lime and borosilicate glasses [1-5]. There have, however, been other applications of electrically poled glasses in the literature. These include using a poled glass layer in order to produce buried optical waveguides [6-10] and surface channel waveguides [9,10]. Poled glass has also been used to manufacture diffractive phase masks [11,12] and to control the size of metallic nanoparticles in glass in an image replication process [11]. The production of nano-surface structures and as a smart substrate with controlled surface reactivity are other applications [13-15]. Poled glass has also been investigated as a method of controlling the permittivity and reducing microwave losses of co-planar waveguides on glass [16]. The micro-mechanical properties of poled glass have also recently been investigated [17].

It is generally accepted that poling of glass with a large applied electric field results in the formation of a region beneath the anode that is depleted of Na^+, K^+ and other mobile positive ions [5,18-19]. Due to the removal of these, a negative space charge develops in the poled region. Depending on the type of anode used, this space charge can be neutralized in a number of ways. For so called blocking anodes, which cannot inject neutralizing positive ions, the applied voltage is dropped across the narrow space charge region thus creating a large electric field. This high field encourages the motion of non-bridging O^- ions towards the anode [5,18]. In the other extreme for non-blocking anodes, the injection of H^+ and OH_3^+ ions from the atmosphere can occur [20]. These replace the Na^+ and K^+ ions that have vacated the poled glass region in a process similar to electric field assisted ion exchange. However, even with this type of anode there is evidence that some oxygen ion motion can occur under certain poling conditions [5].

A number of experiments show composition profiles where the poled glass region is void of Na^+, K^+ and other ions [3, 7, 19]. Being of much lower mobility than Na^+ ions, K^+ and other ions build up in the substrate glass just below the poled region [3,7].

The measurement of the refractive index (RI) of poled glass is limited in the literature. Early work by Carlson and co-workers [19] showed that using spectral reflectivity measurements, the index of a silicate glass reduced from 1.562 to 1.463 after poling with a blocking anode. Since the poled layer mainly consists of Si and O in a silica type network, the index was closer to that of quartz (1.46) than the original glass. Marguillis and co-workers measured the RI of soda-lime glass poled with an Al anode using a scanned reflectivity method [9]. They deduced a reduction in index of 0.023 for a soda-lime glass. The index of a poled soda-lime glass has also been measured using a standard Abbe refractometer [21]. These results indicated a RI between 1.51 and 1.46 but with large error bars due to difficulties in

distinguishing the light-dark transition necessary for measurement. Recent work on poled V073 glass, a borosilicate glass with similar in composition to BK7, reports a reduction in index of 0.02 measured by interferometric methods [11]. Most of the above reports assume a poled glass region with a constant refractive index.

The RI profile within the poled region of a thermally poled sodium rich boro-phosphate-niobate glass has been deduced using micro-infrared reflectance spectroscopy [22]. The authors modelled the RI profile with an exponential decay function although the composition profiles showed a step like Na^+ profile. The current author recently measured the RI profile in electrically poled BK7 glass using an interferometric technique [23]. This showed a relatively constant RI in the poled glass region. The pile-up of low mobility K^+ ions just below the poled glass layer was also observed as a corresponding local increase in the RI.

Due to the removal of ions from the poled layer its glass network undergoes structural rearrangement resulting in a compaction of the layer [14,19]. This compaction will be restrained in the transverse directions by the substrate glass, hence tensile stresses are expected to develop in the poled layer and should be observable as a birefringence.

In this paper we show that the RI and thickness of electrically poled glass can easily be obtained by the analysis of leaky modes. These modes are supported by the poled glass layer and can be accurately measured when light is coupled into the glass by a prism coupling arrangement. The method has utility in that prism coupling is a quick, non-destructive and sensitive method of determining index data. We show that for our samples a fairly featureless step like RI profile is obtained for the poled glass. We confirm the method by measuring the RI profile using an interferometry method. We also compare the poled glass thickness with electrical data obtained during the poling process. Finally we estimate the stress in the poled glass layer from the birefringence of the poled glass obtained from the leaky mode data.

2. EXPERIMENTAL

A. POLING

In this study painted graphite electrodes were used both for the anode and the cathode thereby producing a non-blocking type electrode [20]. A soda-lime glass (Menzel-Gläser microscope slides) 0.8 to 1 mm thick whose composition is shown in table 1, was studied [14]. The painted graphite layers were allowed to dry in air before being placed in the pre-heated tubular furnace set at 261°C. The samples typically took ~45 min in the furnace before reaching a steady-state temperature, after which the power supply was turned on. Fig. 1 shows the electrical arrangement for poling. Electrical poling of soda-lime glass with low impedance power supplies can result in thermal runaway effects. This can be reduced by applying the supply voltage in increasing steps [9]. An alternative is to supply the voltage from a higher impedance supply. In our experiments poling was performed with a high voltage power supply (0-3kV) with an internal resistance of ~3.5 MΩ, in series with which was added a resistance R_S that was either 5 or 10 MΩ. The maximum poling current density was 0.42 Am^{-2}.

Table 1

Oxide	SiO_2	Na_2O	CaO	MgO	K_2O	Al_2O_3	SO_3	Fe_2O_3
Weight %	72.20	14.30	6.40	4.30	1.20	1.20	0.3	0.03

The composition was obtained from [14] and Menzel-Gläser microscope slide data sheet.

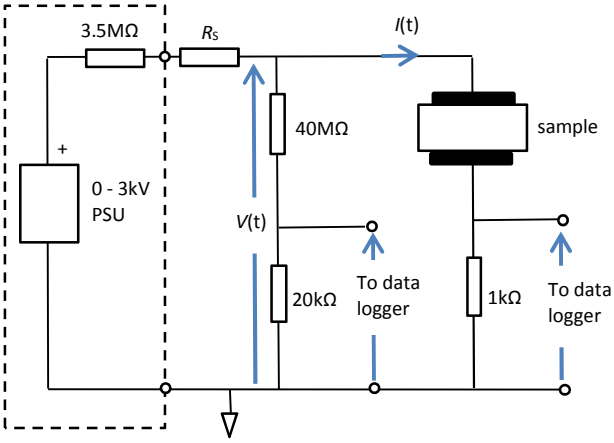

Fig. 1. Electrical arrangement for poling glass samples

The poling voltage, $V(t)$, across the sample increases during the poling procedure as the current decreases and was monitored, via a potential divider, with a data logger. The final poling voltage was between 100V to 400V depending on the poling time. The poling current, $I(t)$, was also logged during the poling process by monitoring the small voltage developed across a 1 kΩ resistance in series with the sample. The voltage drop across this resistance was small in comparison to $V(t)$ and was ignored. The sample was removed from the furnace at the end of the poling process and allowed to cool rapidly with the power supply connected. The charge transported during the poling process, $Q(t)$ was obtained by numerically integrating $I(t)$. Fig. 2 shows a typical plot of the current-time and voltage-time during poling.

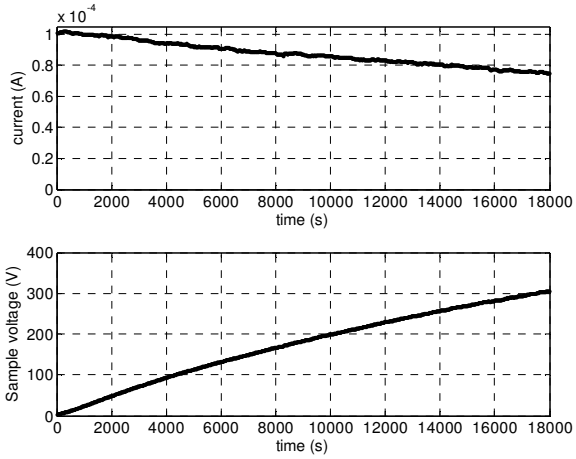

Fig. 2. Electrical data

B. PRISM COUPLING MEASUREMENTS

Prism coupling is an established method of obtaining RI data of ion exchanged layers that support conventional guided modes [24]. However, since the RI of the poled glass is less than that of the substrate glass, conventional guided modes are not supported by these layers. However, we have observed that leaky waveguide modes can be supported and measured if the poled glass layer is sufficiently thick and that these modes can be used to extract quantitative information about the poled glass layer. Here we use the term leaky modes to denote modes that propagate without total internal reflection at the interface between the poled glass and substrate [25-27]. Hence the optical field is continuously lost at each reflection at this interface since the modulus of the reflection coefficient is less than unity. The term leaky modes is also used in the literature when discussing waveguides that do support guided modes but where the field of the guided mode leaks out of the waveguide into the substrate via a dielectric barrier [28,29]. The excitation of a leaky mode by launching light through the substrate into a poled glass layer has also been used to enhance the optical interaction with Au-nanoparticles in a cover layer [30].

Fig. 3 shows a diagram of the prism coupling arrangement used. The high index prism has a base dimension of 5mm x 5mm. This is sufficiently small such that it is possible to press it against the sample and obtain optical coupling without the use of an index matching fluid. Two detectors D_R and D_T in fig. 3 can detect reflected power and transmitted power along the poled glass layer. The prism coupler uses a He-Ne laser at a wavelength λ = 543.5 nm.

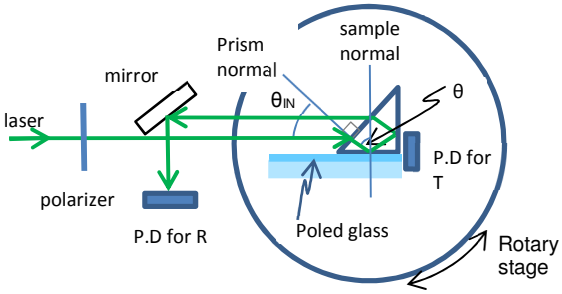

Fig. 3. Experimental arrangement for the measurement of mode spectra (colour on-line).

Fig. 4 shows a reflection spectrum obtained on the anode side for a typical poled sample. For comparison purposes, a spectrum obtained for an un-poled sample and one obtained for quartz are also shown. These spectra have been normalized by dividing them by the reflected power as a function of angle that is obtained without a sample pressed against the prism. Rather than plotting the spectra against the input angle θ_{IN} of fig. 3, the spectrum is plotted as a function of the effective refractive index $n_e = n_p \sin\theta$ where θ is the angle of propagation with respect to the normal to the prism base and n_p is the index of the prism. For the un-processed glass and quartz, if n_e is greater than n_s, the substrate index, then light is totally internally reflected at the prism base and hence the reflectivity is unity. The changes in reflectivity highlighted in fig. 4 for the unprocessed glass and quartz thus correspond to their bulk refractive indices. The poled soda-lime glass reflectivity spectrum is significantly different to the un-poled sample with sharp minima in the reflectivity being observed, which reduce in sharpness as n_e is reduced. The minima are well below the RI of the unprocessed soda-lime glass, hence indicating that the index of the poled glass has been reduced. The minima correspond exactly to peaks in the transmission spectrum detected by D_T and correspond to the angles where the leaky modes are supported by the layer. There were no noticeable differences between the reflectivity spectrum measured on the cathode side of the samples and that of unprocessed glass.

In none of the samples produced were normal optical modes observed with n_e greater than the substrate index n_s of the unprocessed soda-lime glass. These normal modes have been observed in other work on poled glass and can be attributed to buried waveguide formation due to the pile-up outside the poled glass region of low mobility ions (K^+, Ca^{++}) depending on the composition [7]. The inability to excite these modes can be attributed to the thickness of the poled glass layers in our work, the low K^+ ion concentration in our glass and the lack of Ca^{++} ion motion, as will be discussed.

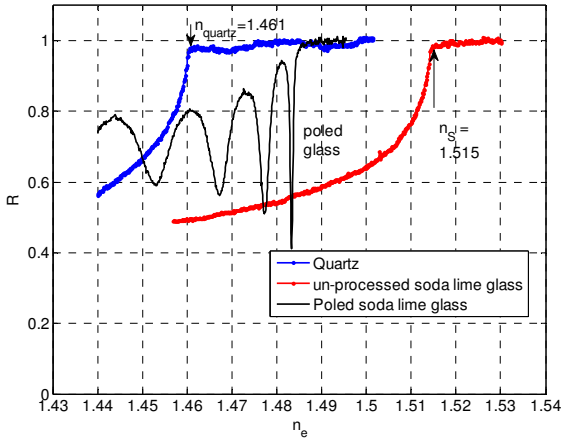

Fig. 4. Comparison of TE reflection spectrum obtained from prism coupling measurements for poled soda-lime glass, un-poled soda-lime glass and un-poled Quartz. (colour on-line)

The RI depth profile on the anode side was also obtained using an interferometric technique previously outlined [23]. The method involves polishing a shallow bevel (typically 4° to 6°) in the glass surface through the poled glass region and placing the sample together with an index matching oil on an optical flat in one arm of an interferometer. A measurement wavelength of 546 nm was used and is close to that used in the prism coupling measurements. The information about the index profile is contained in the spatial derivative of the phase of the interferogram. The details of the numerical techniques used to extract the index data from the interferogram are discussed elsewhere [23].

3. SIMPLE REFLECTIVITY ANALYSIS

Reflectivity measurements have been used to analyse other material systems including ion implanted insulators and deposited layers [28,29,31]. The interpretation of reflectivity spectra can be done in a number of ways depending on the level of sophistication of the index model used. The simplest is to assume a step index profile with a constant index n_{poled} for the poled glass layer of thickness d stepping up to the substrate index. By considering the round trip phase delay in a direction

normal to the surface and requiring this to be is a multiple of 2π, the reflectivity minima will occur when

$$\frac{4\pi d}{\lambda}\sqrt{n_{poled}^2 - n_e^2(m)} = m2\pi + \varphi_1 + \varphi_2 \quad \textbf{(1)}$$

where m is an integer = 0,1,2..., and φ_1 and φ_2 are the phase changes at the poled glass-air interface and poled glass-substrate interfaces respectively. For the poled glass-air interface where total internal reflection occurs φ_1 is given by

$$\varphi_1 = 2\tan^{-1}\left\{r\sqrt{\frac{n_e^2-1}{n_{poled}^2-n_e^2}}\right\} \quad \textbf{(2)}$$

where r=1 for TE propagation and $r = n_{\text{poled}}^2$ for TM propagation [26,32]. It is common in the analysis of guided modes to approximate eqn. (2) to π radians [29], which will be valid if $n_e \cong n_{poled}$. Since $n_{\text{poled}}<n_s$ total internal reflection does not occur at the poled glass-substrate interface and thus the phase change φ_2 = π for TE modes for all propagation angles, i.e. for all n_e [32]. For TM propagation, φ_2 = π for propagation angles greater than the Brewster angle $\theta_B = \tan^{-1} n_S/n_{poled}$. Since the index change between poled glass and substrate is relatively small, the Brewster angle will be close to 45°. Propagation angles within the poled glass region are all greater than this, hence a phase change of π radians is again appropriate. Hence setting $\varphi_1 = \pi$ and $\varphi_2 = \pi$ in eqn. (1) gives

$$n_e^2(m) = n_{poled}^2 - \left(\frac{\lambda}{2d}\right)^2 (m+1)^2 \quad \textbf{(3)}$$

Fig. 5 shows a plot of a number of poled glass samples using this analysis. A green He-Ne laser at a wavelength λ = 543.5 nm is used From fig. 5 it can be seen that the mode data follows a straight line consistent with eqn. (3), from the slope of which the poled glass layer thickness d can be measured. The poled glass index n_{poled} can also be obtained from the intercept $(m+1)^2 = 0$. If we extrapolate the mode data to $(m+1)^2 = 0$ in fig. 5 we estimate that n_{poled} is between1.486 and 1.487.

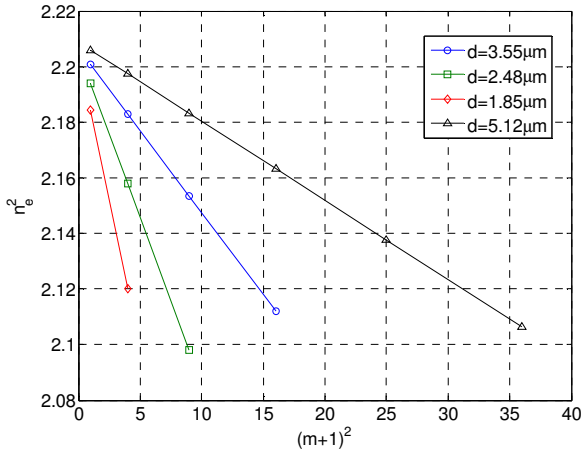

Fig. 5. Plot of square of measured effective refractive index n_e^2 of leaky modes *vs* $(m+1)^2$ for a number of poled glass samples (colour on-line).

In order to assess the significance of the approximation made for φ_1, in fig. 6 model data is plotted for a step index profile of known depth using eqn. (2) with and without the approximation. The difference in actual and measured depth deduced from the slopes in the TE and TM lines and the approximation is less than 2.5%. It can also be seen that the lines converge when $(m+1)^2$=0, which shows that a value of n_{poled} deduced from the extrapolation will be the same.

In order to confirm these measurements the index profile was obtained using the interferometer method [23]. Fig. 7 shows the index profile obtained using this method for a typical sample. A fairly uniform refractive index in the poled region and a sharp transition between the poled glass and bulk can easily be observed in the profile. Fig. 7 also shows the profile obtained from the reflectivity analysis for this sample, which is in good agreement.

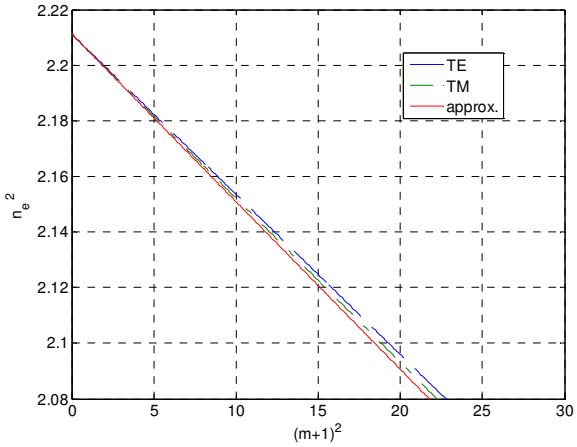

Fig. 6. Plot based on calculation comparing approximation (solid) with exact solution of eqn. (2) for TE and TM modes. d=3.5μm, n_{poled}=1.487, (colour on-line).

For the poling of BK7 glass with a relatively high K^+ concentration it was possible to observe with the interferometer method an increase in the index due to the K^+ pile-up region [23]. However, in the soda-lime glass samples used in this study this is hardly observable in fig. 7 due to the low K^+ ion concentration (table 1).

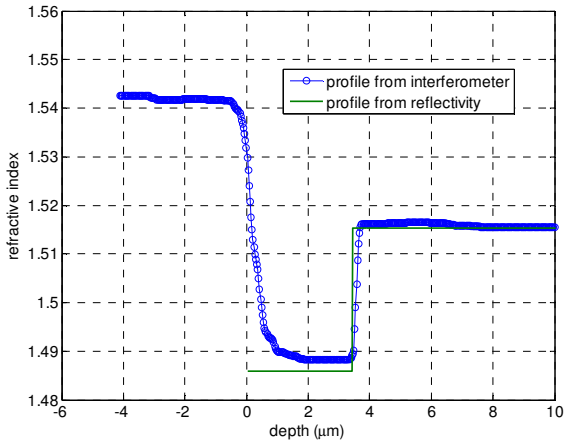

Fig. 7. Comparison between index profile of a sample obtained from interferometry and that obtained from leaky mode spectrum (colour on-line).

4. REFLECTIVITY MODELLING

A more sophisticated analysis of the reflectivity data can be performed by calculating the reflectivity spectra for a given model index profile and fitting its parameters such that the

theoretical and measured experimental reflectivity spectra coincide. This is necessary if the poled glass layer is thin and supports only a few or even just one leaky mode. A number of matrix methods have been published in the literature that can calculate the reflectivity spectra [28,29,31,33]. The theoretical reflectivity spectra $R(\theta)$ is calculated using a standard matrix method [33] whereby the glass is divided into a large number N of layers of constant refractive index that are lossless. If we denote the incident and reflected electric field in the prism by E_1^+ and E_1^- and those in the substrate by E_N^+ and E_N^- then these are related by

$$\begin{pmatrix} E_1^+ \\ E_1^- \end{pmatrix} = \boldsymbol{M} \begin{pmatrix} E_N^+ \\ E_N^- \end{pmatrix} \quad \textbf{(4)}$$

The matrix $\boldsymbol{M}$ is given by

$$\boldsymbol{M} = \boldsymbol{M}_1 . \boldsymbol{M}_2 \ldots \ldots \boldsymbol{M}_N \quad \textbf{(5)}$$

where the matrix of the jth layer, $\boldsymbol{M}_j$, is given by

$$\boldsymbol{M}_j = \frac{1}{t_{j+1}} \begin{pmatrix} e^{i\delta_j} & r_{j+1}e^{i\delta_j} \\ r_{j+1}e^{-i\delta_j} & e^{-i\delta_j} \end{pmatrix} \quad \textbf{(6)}$$

where r_{j+1} is the Fresnel reflection coefficient and t_{j+1} is the Fresnel transmission coefficient at the j, j+1 th interface, $\delta_j = \frac{2\pi}{\lambda} n_j \cos\theta_j . d_j$. The angle θ_j is the propagation angle in the j^{th} layer with respect to the surface normal. The angle θ_1 (= θ) is related to the angle θ_{IN} shown in fig. 3, the prism index and the prism base angle [24]. Layer 1 corresponds to the prism of index n_p and layer 2 corresponds to the air gap of size x_g between the prism and glass, which is unknown and one of the adjustable parameters in the fitting procedure. The reflectivity calculated in the prism, $R(\theta)$ is given by $|E_1^-/E_1^+|^2$ when $E_N^-=0$. $R(\theta)$ can also be determined experimentally since the measured reflection coefficient $R_D(\theta)$ is given by

$$R_D(\theta) = H(\theta)T_{ap}(\theta)T_{pa}(\theta)R(\theta) \quad \textbf{(7)}$$

where $T_{ap}(\theta)$ and $T_{pa}(\theta)$ are the air to prism and prism to air transmittivity and $H(\theta)$ is the instrumentational transfer function [31]. Without the sample pressed against the prism $R(\theta)$=1 so the measured reflection coefficient for this experimental situation is

$$R_{D,O}(\theta) = H(\theta)T_{ap}(\theta)T_{pa}(\theta) \quad \textbf{(8)}$$

$R_{D,O}(\theta)$ is a slowly varying featureless function of θ. Hence from (7) and (8), $R(\theta)$ can be determined from experimental data by taking the ratio

$$R(\theta) = \frac{R_D(\theta)}{R_{D,O}(\theta)} \quad \textbf{(9)}$$

We assume a model index profile when calculating $R(\theta)$ of the form

$$n(z) = n_s - \frac{\Delta n}{1+\exp\{\frac{z-d}{a}\}} \quad \textbf{(10)}$$

where n_s is the substrate index for the glass, and Δn, d and a together with the prism air gap, x_g are adjustable parameters. The parameter $\Delta n = n_s - n_{poled}$ represents the index difference between the un-poled and poled glass, d is the poled layer thickness and the slope parameter, a, characterizes the steepness of the transition from poled to un-poled glass. As the parameter a tends to zero, the index profile tends to a step profile. The mean of the square of the difference between the reflectivity spectrum calculated from the matrix method, $R(\theta)$, and the experimental reflectivity spectrum, deduced from eqn. (9), is calculated. This is minimized by adjustment of the model parameters in a direct search algorithm. Estimates from plots shown in fig. 5 provide good initial guesses for Δn and d if available.

It is useful to observe how the four adjustable parameters, d, Δn, a and x_g affect the model reflectivity spectrum. This is shown in fig. 8 to 11 where each parameter is adjusted separately. It can be seen from fig. 8 that altering d alters the spacing between the reflectivity minima. From fig. 9 it can be seen that changing Δn effectively shifts the spectrum along the n_e axis. Fig. 10, shows that x_g alters the average level of the spectrum along the R axis and that the perturbing effect of the prism on the n_e values at the minima is quite small.

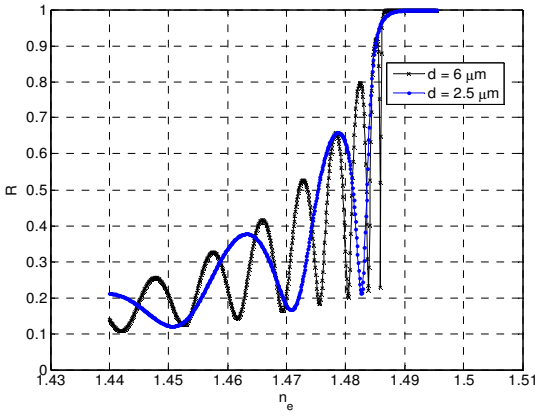

Fig. 8. Showing effect of change of guide depth, d, on reflectivity spectra. Δn =0.0284, n_s=1.515, n_p=1.6525, a =0.05 μm, x_g=0.01 μm (colour on-line).

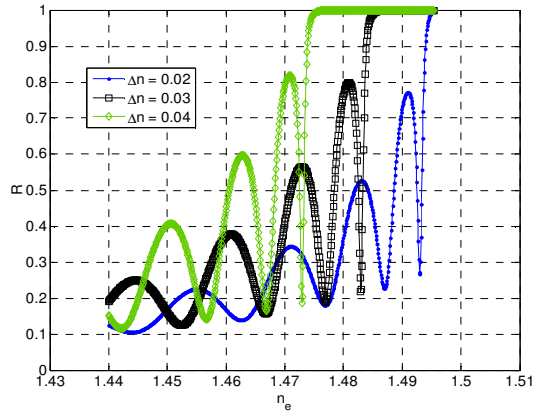

Fig. 9. Showing effect of index change Δn on reflectivity spectra. d=3.5μm, n_s=1.515, n_p=1.6525, a =0.05 μm, x_g=0.01 μm (colour on-line).

Finally from fig 11 it can be seen that transition parameter, a, alters the contrast of the reflectivity minima. A large value of a, corresponding to a long transition from poled to un-poled glass, causes the reflectivity spectra minima to disappear. Using the index model in eqn. (10), the index change from (n_s-0.9Δn) to (n_s-0.1Δn) occurs in a distance of 4.4a. Thus, as expected, the plot in fig. 11 shows that in order to observe the leaky mode spectrum a transition between the poled and un-poled glass over a distance of a wavelength or less is required.

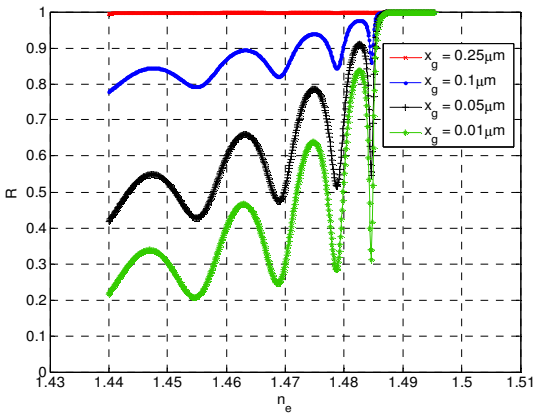

Fig. 10. Showing effect of air gap distance x_g on reflectivity spectra. d=3.5µm, Δn =0.0284, n_s=1.515, n_p=1.6525, a =0.05µm (colour on-line).

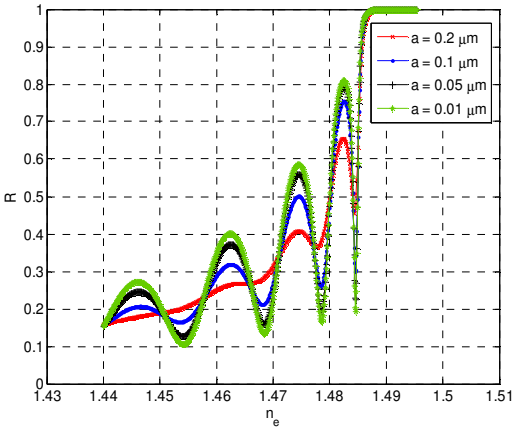

Fig. 11. Showing effect of Fermi slope parameter a on reflectivity spectrum. d=3.5µm, Δn=0.0284, x_g=0.01µm, n_s=1.515, n_p=1.6525 (colour on-line).

Fig. 12 compares a typical experimental reflectivity spectrum with that obtained from the fitting algorithm. The parameters deduced from the fitting are given in the caption. The slope parameter, a, has iterated to a very small value indicating an almost step index profile. It can be seen that the positions of the leaky mode minima are well modelled, although the relative intensity of the two spectra differs somewhat for small n_e. This indicates that a slightly more sophisticated refractive index model than eqn. (10) may be required. The values of d and Δn deduced from the fitting algorithm are very close to those obtained from the eqn. (3), which assumes a step index profile.

It was possible, using the fitting algorithm, to determine the depth and index change of a very shallow poled glass layer of 1.28µm depth that had only one measurable leaky mode. The fitting process gave Δn = 0.03 for this sample consistent with the other samples.

5. ION MOTION CONSIDERATIONS

The thickness, d, of the poled glass layer is expected to increase linearly with the charge transported during the poling process, Q. Fig. 13 plots d, determined optically, *vs* Q/A where A is the anode electrode cross sectional area. Fig. 13 contains data points deduced from the reflectivity data and it can be seen that the linear increase is confirmed. If we assume that both Na^+ and K^+ ions are removed from the poled glass region of thickness d, then equating the charge removed with the measured charge during the poling process we obtain

$$d = \frac{Q}{eA(C_{Na}+C_K)} \qquad \textbf{(11)}$$

where C_{Na} and C_K are the Na^+ and K^+ ion concentrations. A line based on eqn. (11) is shown in fig. 13. It can be seen that there is reasonable agreement between the experimental data and this line which supports the assertion that most Na^+ and K^+ ions have been removed from the poled glass region. The soda lime glass also contains Ca, which exist as doubly charged ions in the glass. Based on the composition in table 1, it can be deduced that the gradient of the line in fig. 13 would be reduced by a factor 0.68 if the Ca^{++} ions were also mobile. The line assuming only Na^+ and K^+ mobile ions fits the data reasonably well, indicating that the Ca^{++} ions are effectively immobile at the temperature and fields used in this investigation.

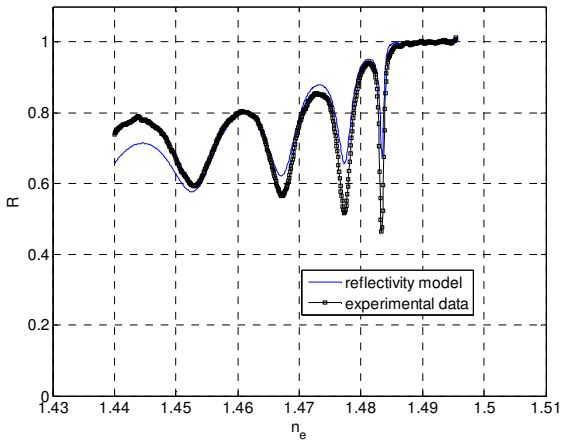

Fig. 12. Comparison of experimental reflectivity spectra (line with squares) with Fermi function model (solid). Model parameters for Fermi function d =3.43µm, Δn = 0.0296, a=6.25x10^{-5} µm, x_g =0.071 (colour on-line).

From simple drift and diffusion ion motion models, a sharp transition in RI between poled and un-poled glass is to be expected. Assuming a non-blocking anode and assuming complete replacement of Na^+ by H^+ then a H^+ concentration profile C_H of the form

$$C_H = \frac{C_{Na}}{1+exp\left\{\frac{(1-M)J}{eD_H C_{Na}}(x-d)\right\}} \qquad \textbf{(12)}$$

is predicted where J is the current density at the end of the poling process, D_H is the diffusion coefficient and M=μ_H/μ_{Na} is the mobility ratio [34]. Hence the model predicts a slope parameter

$$a \cong \frac{eD_H C_{Na}}{(1-M)J} \qquad \textbf{(13)}$$

Using the Einstein relation, $D_H = \mu_H KT/e$ and assuming that most of the applied voltage V is dropped across the poled glass region, then $J = e\mu_H C_{Na} V/d$, thus

$$a \cong \frac{1}{1-M}.\frac{KT}{e}.\frac{d}{V} \qquad \textbf{(14)}$$

Using M~10^{-3} [5], V=300V and d = 5µm we estimate a~10^{-3} µm, which is clearly a very small value. The model in eqn. (12)

ignores the effect of K^+ ions. Analytical models that include their effect are not available at present.

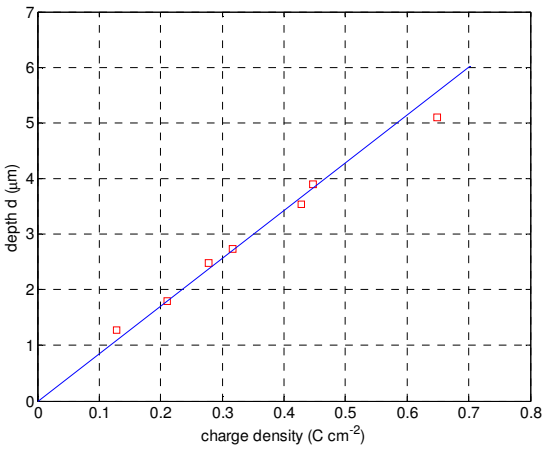

Fig. 13. Poled glass depth *d vs* injected charge density. Squares are experimental reflectivity data. Solid line based on soda-lime glass composition (colour on-line).

6. BIREFRINGENCE MEASUREMENTS

Poled glasses layers are expected to compact due to the removal of ions from the layer [14]. Although compaction of the glass network occurs, it will be restrained in the transverse directions by the substrate glass, hence tensile stress is expected to develop in the poled layer. Via the stress optical effect, the stress should be observable in a birefringence in the RI. We first note from fig. 6 that there is, even without stress effects, a small difference between the TE and TM modes due to the difference in the phase change term φ_1. However, from fig. 6 although the gradients of the TE and TM slopes are slightly different they converge to the same surface index value. However, it can be seen in fig. 14 that the practical TE and TM data does not converge to the same index and that $n_{poled}^{TE} > n_{poled}^{TM}$ indicating a tensile stress. From this plot the birefringence is estimated to be $n_{poled}^{TE} - n_{poled}^{TM} \cong 7 \times 10^{-4}$. The magnitude of the stress in the poled glass layer, σ, is estimated by

$$\sigma = \frac{n_{poled}^{TE} - n_{poled}^{TM}}{C_2 - C_1} \qquad \textbf{(15)}$$

where the stress optical coefficient $C_2 - C_1$ =2.38x10^{-12} m^2/N is obtained from the literature for glass of the same composition [35]. This gives σ~0.3 GN/m^2, which is slightly less in magnitude than the compressive stress typically obtained for K^+ ion exchange experiments in soda-lime glass (-0.7 to -1 GN/m^2). It should be emphasized that the stress is approximate since we are using stress optical coefficients of the un-poled glass for a poled glass layer. Micro cracks are observable in our sample with Q/A ~0.65 C/cm^2, which is further evidence of a tensile stress. Between the micro cracks the glass is continuous. Micro cracks together with other defects have been observed in the same glass but with very different poling conditions [14]. In those experiments poling was performed with a different anode and the sample voltage was applied in steps. The point and line defects observed were attributed to the enhanced attraction of the anode material to the glass as poling proceeded. This resulted in the anode becoming a blocking type resulting in the removal of oxygen ions from the glass and causing additional compaction [14].

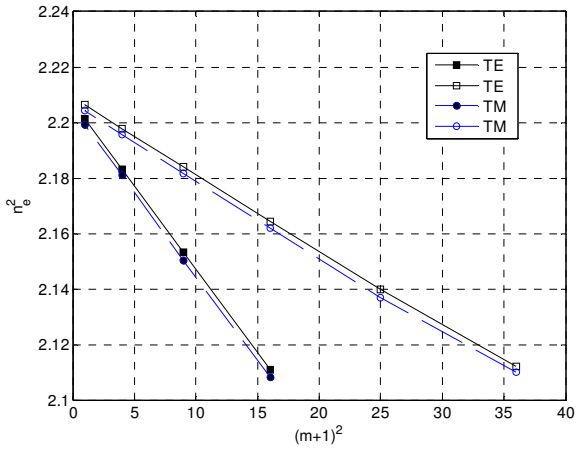

Fig. 14. Plot of square of effective refractive index n_e^2 of TE and TM leaky modes *vs* $(m+1)^2$ showing birefringence for two samples (colour on-line).

7. CONCLUSIONS

Poled soda-lime glass layers have been produced with graphite anodes in an air atmosphere. The poled glass depth and RI have been measured by the analysis of leaky modes using a prism coupler and confirmed using interferometry. The two methods of assessment agree well with each other and show a poled glass layer of constant refractive index of value 1.487. The fact that leaky modes can be observed in the reflectivity data itself indicates that the transition between poled and un-poled glass is very rapid and over a distance clearly less than the wavelength of light. A comparison of the depth data with electrical data obtained during the poling indicates the removal of all Na^+ and K^+ ions from the poled glass layer. An estimation of the tensile stress in the poled glass layer has been made from the observed birefringence of the RI in the poled layer and gives a value ~0.3GN/m^2. For deep poled glass layers the tensile stresses that develop can cause micro cracks to appear in the poled glass layer.

Finally we note that the analysis of poled glass layers using leaky modes excited by a prism coupler is a fast and non-destructive technique. Prism coupling has typically an index resolution of ~10^{-4} [35] and thus it could potentially be used as a convenient and sensitive method to assess the long term stability of poled glass layers.

References

1. M. Dussauze, T. Cremoux, F. Adamietz, V. Rodriguez, E. Fagin, G. Yang and T. Cardinal "Thermal poling of optical glasses: Mechanisms and second-order optical properties" Int. J. of Applied Glass Science **3** 309-320 (2012)
2. H. An and S. Fleming "Second-order nonlinearity in thermally poled borosilicate glass" Appl. Phys. Lett. **89** 181111 (2006)
3. H. An and S. Fleming "Second-order optical nonlinearity and accompanying near-surface structural modifications in thermally poled soda-lime silicate glasses." J. Opt. Soc. Am. B **23** 2303-2309 (2006)

4. H. An and S. Fleming "Near-anode phase separation in thermally poled soda lime glass" Appl. Phys. Lett. **88** 181106 (2006)
5. M. Dussauze, V. Rodriguez, A. Lipovskii, M. Petrov, C. Smith, K. Richardson, T. Cardinal, E. Fargin and E. I. Kamisos "How does poling affect the structure of soda-lime glass?" J. Phys. Chem. C **114** 12754-12759 (2010)
6. T. Kaneko T "A diffusion technique for producing an inside-maximum distribution of refractive index in glass plates" Opt. Comm. **52** 17-23 (1984)
7. A.L.R. Brennand and J.S. Wilkinson "Planar waveguides in multicomponent glasses fabricated by field-driven differential drift of cations." Opt. Lett. **27** 906-908 (2002)
8. K. Liu and E.Y.B. Pun "Buried ion-exchanged glass waveguides using field assisted annealing." IEEE Photonics Technology Letters **17** 76-78 (2005)
9. W. Margulis and F. Laurell "Fabrication of waveguides in glasses by a poling procedure" Appl. Phys. Lett. **71** 2418-2420 (1997)
10. I.C.S. Carvalho, M Fokine, C.M.B. Cordeiro, H Carvalho and R. Kashyap "Borosilicate glass for photonic applications." Opt. Mat. **30** 1816-1821 (2008)
11. A. Lipovskii , V.V. Rusan and D.K. Tagantsev "Imprinting phase/amplitude patterns in glasses with thermal poling." Solid State Ionics **181** 849-855 (2010)
12. L.A.H. Fleming, D.M. Goldie and A. Abdolvand "Imprinting of glass" Opt. Mat. Express **5** 1674-1681 (2015)
13. P.N. Brunkov, V.G. Melekhin, V.V. Goncharov, A.A. Lipovskii and M.I. Petrov "Submicron-Resolved Relief Formation in Poled Glasses and Glass-Metal Nanocomposites" Tech. Phys. Lett. **34** 1030-1033 (2008)
14. A.V. Redkov, V.G. Melehin, V.V. Statcenko and A.A. Lipovskii "Nanoprofiling of alkali-silicate glasses by thermal poling" J. Non-Cry. Solids. **409** 166-169 (2015)
15. A. Lepicard, T. Cardinal, E. Fargin, F. Adamietz, V. Rodriguez, K. Richardson and M. Dussauze "Surface Reactivity control of a borosilicate glass using thermal poling" J. Phys. Chem. C **119** 22999-23007 (2015)
16. R. Oven and P.R. Young "Microwave loss of coplanar waveguides on electrically ion depleted borosilicate glass." IEEE Microwave and Wireless component Letters **15** 125-127 (2005)
17. H. He, J. Luo, L. Qian, C.G. Pantano and S.H. Kim "Thermal poling of soda-lime silica glass with non-blocking electrodes – Part 2: Effects on Mechanical and Mechanochemical Properties" J. Am. Ceram. Soc. **99**, 1231-1238 (2016)
18. D.E. Carlson "Ion depletion of glass at a blocking anode: 1, Theory and Experimental Results for alkali silicate glasses." J. Am. Ceram. Soc. **57** 291-294 (1974)
19. D.E. Carlson, K.W. Hang and G.F. Stockdale "Ion depletion of glass at a blocking anode: 2, Properties of ion depleted glass." J. Am. Ceram. Soc. **57,** 295-300 (1974)
20. D.E. Carlson "Anodic proton injection in glasses." J. Am. Ceram. Soc. **57**, 461-466 (1974)
21. E.C. Ziemath, V.D. Araujo and C.A. Escanhoela "Compositional and structural changes at the anode surface of thermally poled soda-lime float glass." J. Appl. Phys. **104** 054912 (2008)
22. M. Dussauze, E.I. Kamitsos, E. Fargin and V. Rodriguez "Refractive index distribution in the non-linear optical layer of thermally poled oxide glasses." Chem. Phys. Lett. **470** 63-66 (2009).
23. R. Oven "Measurement of planar refractive index profiles with rapid variations in glass using interferometry and total variation regularized differentiation" J. Mod. Opt. **62**, S59-S66, (2015).
24. S.I. Najafi (Ed) "Introduction to Glass Integrated Optics" Artech House (Boston, London) 1992 ISBN 0-89006-5470
25. R.T. Kersten "The prism-film coupler as a precision instrument Part 1 Accuracy and capabilities of prism couplers as instruments" Opt. Acta **22** 503-513 (1975)
26. T.N. Ding and E. Garmire "Measurement of thin film parameters using substrate excitation of leaky modes'. Opt. Comm. **48** 113-115 (1983)
27. A.B. Sotsky, L.M. Steingart, J.H. Jackson, P Ya. Chudakovskii and L.I. Sotskaya "Prism excitation of leaky modes of thin films" Tech. Phys. **58** 1651-1660 (2013)
28. P.D. Townsend, P.J. Chandler and L. Zhang "Optical effects of ion implantation" Cambridge Studies in Modern Optics ISBN 0-521-39430-9 (1994)
29. P. Mathey, P. Jullien and J.L. Bolzinger "Refractive-index profile reconstructions in planar waveguides by the WKB inverse method and reflectivity calculations" J. Opt. Soc. Am. B **12** 1663-1670 (1995)
30. C. Corbari, M. Beresna, O. Deparis and P.G. Kazansky "Leaky-modes excitation in thermally poled nanocomposite glass and their exploitation for saturable absorption" in Advanced Photonics and Renewable Energy, OSA Technical Digest (CD), paper BTuB7 (2010)
31. J. Cardin and D. Leduc "Determination of refractive index, thickness, and the optical losses of thin films from prism-film coupling measurements" Appl. Opt. **47** 894-900 (2008)
32. D.L. Lee Electromagnetic Principles of Integrated Optics 1986 ISBN 0-471-879778-9 (New York) Wiley
33. O.S. Heavens Optical Properties of thin solid films Dover (New York) 1965
34. X. Prieto and J. Linares, "Increasing resistivity effects in field-assisted ion exchange for planar optical waveguide fabrication" Opt. Lett. **21** 1363 (1996)
35. A. N. Miliou, R. Srivastava and R.V. Ramaswamy, "Modeling of the index change in K^+-Na^+ ion-exchanged glass" Appl. Opt. **30** 674-681 (1991)